FUSION

Vera Andrejchenko [a], Rob Heylen [a], Paul Scheunders [a], Wilfried Philips [b], Wenzhi Liao [b]

Visionlab, University of Antwerp [a]

Image Processing and Interpretation, University of Gent [b]

ABSTRACT

Index Terms— unmixing, supervised classification, fusion

1. INTRODUCTION

2. METHOD

In this section, we propose two approaches for fusion of abundance fractions produced by an unmixing method and probability outputs from a supervised classifier. The ultimate goal is to improve the overall accuracy including complementary information from both decision sources in the case of low number of training pixels. Let n be the total number of reflectances, $D = \{(\mathbf{x}_i, y_i)\}_i$ with $i = 1, \ldots, m$ be the labeled training data and $T = \{(\mathbf{x}_j, y_j)\}_j$ with $j = 1, \ldots, n$ the test data (the whole image). For modeling of the posterior probabilites we used Multinomial Logistic Classifier (MLR):

$$p(y_i = c|\mathbf{x}_i) = \frac{\exp(\boldsymbol{\beta}_c^T \mathbf{x_i})}{\sum_{c=1}^{C} \exp(\boldsymbol{\beta}_c^T \mathbf{x_i})} \tag{1}$$

where the $\mathbf{x_i}$ is the reflectance vector and $\boldsymbol{\beta} = \left[\boldsymbol{\beta}_1, \boldsymbol{\beta}_2, ...\boldsymbol{\beta}_c\right]$ are the regression coefficients obtained from the training data. Using the estimated $\boldsymbol{\beta}$ coefficients we compute the probabilities for the whole test spectrum, select the maximal probability value and assign the corresponding label to the pixel.

$$\hat{c}_j = arg\max_j p(y_j = c|\mathbf{x}) \tag{2}$$

We compute the abundances with the SunSAL unmixing method, and set the complete training data as a dictionary of endmembers.

$$\min_y \frac{1}{2}\|\mathbf{E}\boldsymbol{\alpha} - \mathbf{y}\|_2^2 + \lambda\|\boldsymbol{\alpha}\|_1, \qquad \text{s.t.}\boldsymbol{\alpha} \geq 0. \tag{3}$$

Here also we select the maximum abundance value and assign the corresponding label to the i-th test spectrum.

$$\hat{c_j} = arg\max_j \boldsymbol{\alpha}_i \tag{4}$$

Once the individual decisions were obtained from the unmixing and the MLR classifier, we define the fusion problem of our modalities in terms of graphs using MRF and CRF. In the general MRF approach the graph is defined over the class labels $\boldsymbol{y} = \{y_1, y_2, ...y_n\}$ set as nodes in the graph and the following energy function is minimized:

$$E(\mathbf{y}) = -\sum_{i \in V} \ln p(\mathbf{x_i}|y) + \beta \sum_{i \in V, j \in N_i} \psi_{i,j}(y_i, y_j) \tag{5}$$

where $\delta(y_i, y_j)$ is the indicator function $\delta()$, (i.e. $\delta(a, b) = 1$ for $a = b$ and $\delta(a, b) = 0$ otherwise) and $\psi_{i,j} = (1 - \delta(y_i, y_j))$ are the pairwise potentials which are label dependent and impose smoothness on the neighboring labels N_i.

2.1. MRF with cross links for fusion

In our approach we consider nodes from both abundance and probability sub-graphs V_1 and V_2. The energy function is constructed as a linear combination of several contributions:

$$\begin{aligned} E(\mathbf{y}) = &\sum_{i \in V_1} \psi_i^{\alpha}(y_i) + \sum_{i \in V_2} \psi_i^{p}(y_i) \\ +\beta\Big[&\sum_{i \in V_1, j \in N_i} \psi_{i,j}^{\alpha}(y_i, y_j) + \sum_{i \in V_2, j \in N_i} \psi_{i,j}^{p}(y_i, y_j)\Big] \\ &+\gamma \sum_{i \in V_1, j \in V_2} \psi_{i,j}^{\alpha p}(y_i, y_j) \end{aligned} \tag{6}$$

$$\psi_{i,j} = (1 - \delta(y_i, y_j)) \tag{7}$$

Unary potentials from the individual sources defined on single pixels (nodes): ψ_i^{α} - fractional abundance(s) and ψ_i^{p} - probability estimates. As in the general MRF the pairwise potentials from the individual sources are defined on pairs of label nodes encoding spatial (neighborhood) relation: $\psi_{i,j}^{\alpha}$ - spatial

relation (smoothness) between the neighboring labels, where the labels are produced by the abundances, and $\psi^p_{i,j}$ - spatial relation between the neighboring labels, where the labels are produced by the probability estimates. The last term $\psi^{\alpha p}_{i,j}$ is the connecting term applied on both modalities V_1 and V_2, penalizing dissimilar labeling of the corresponding nodes from the sub-graphs. The β weights the contribution to all pairwise potential terms. The interaction between only two label nodes from the different sources, where the individual spatial relation is taken into account is depicted in Fig. 1. In addition, the interaction among all label nodes from these two sources can be seen in Fig 2.

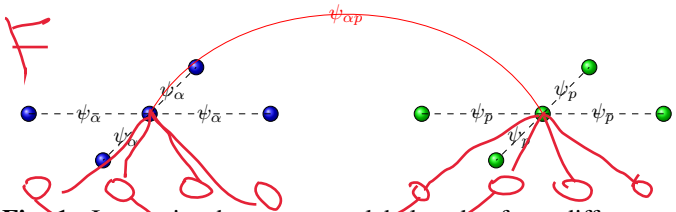

Fig. 1: Interaction between two label nodes from different decision sources. The blue and the green nodes are the label nodes from the abundance source V_1 and probability source V_2, respectively. The red link is the interaction potential between the central blue and central green label node.

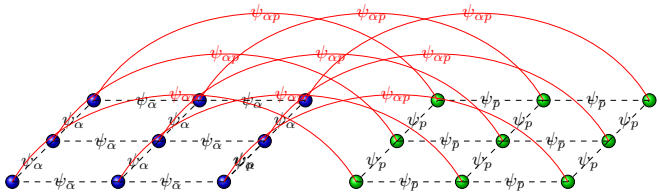

Fig. 2: Interaction between all label nodes from different decision sources. The red links are all the interactions among the nodes from the individual graphs.

2.2. CRF with cross links for fusion

Similarly, we propose a second fusion method which is based on the special form of the MRF. Unlike the MRF, which through the pairwise potentials models the smoothness of the neighboring labels only, the CRF pairwise potentials capture a richer context by directly incorporating the observed data - the abundances and probability estimates in the pariwise potentials and model their smoothness in addition to the label smoothness. A cost is introduced for different labeling depending of the distance between the abundance and probabilities.

$$E(\mathbf{y}) = \sum_{i \in V_1} \psi^{\alpha}_i(y_i) + \sum_{i \in V_2} \psi^{p}_i(y_i) + \beta \Big[\sum_{i \in V_1, j \in N_i} \psi^{\alpha}_{i,j}(y_i, y_j) + \sum_{i \in V_2, j \in N_i} \psi^{p}_{i,j}(y_i, y_j) \Big] + \gamma \sum_{i \in V_1, j \in V_2} \psi^{\alpha p}_{i,j}(y_i, y_j) \quad (8)$$

$$\psi^{\alpha}_{i,j} = \begin{cases} 0 & \text{if } y_i == y_j \\ e^{\frac{-\theta_b \|\boldsymbol{\alpha}_i - \boldsymbol{\alpha}_j\|}{\sigma}} & \text{otherwise} \end{cases} \quad (9)$$

$$\psi^{p}_{i,j} = \begin{cases} 0 & \text{if } y_i == y_j \\ e^{\frac{-\theta_b \|\boldsymbol{p}_i - \boldsymbol{p}_j\|}{\sigma}} & \text{otherwise} \end{cases} \quad (10)$$

$$\psi^{\alpha p}_{i,j} = \begin{cases} 0 & \text{if } y_i == y_j \\ e^{\frac{-\theta_b \|\boldsymbol{\alpha}_i - \boldsymbol{p}_j\|}{\sigma}} & \text{otherwise} \end{cases} \quad (11)$$

Here the pairwise potentials $\psi_{i,j}$ provide a link between the class labels, the observed abundances and probabilities. The pairwise potentials $\psi^{\alpha}_{i,j}$ - represents direct interaction between the neighboring abundances α_i and α_j, and $\psi^{p}_{i,j}$ - direct interaction between the neighboring probabilities p_i and p_j. Whereas the last pairwise potentials: $\psi^{\alpha p}_{i,j}$ produces the connection between the corresponding abundances α_i and probabilities p_j from the individual sub-graphs V_1 and V_2. See Fig 3.

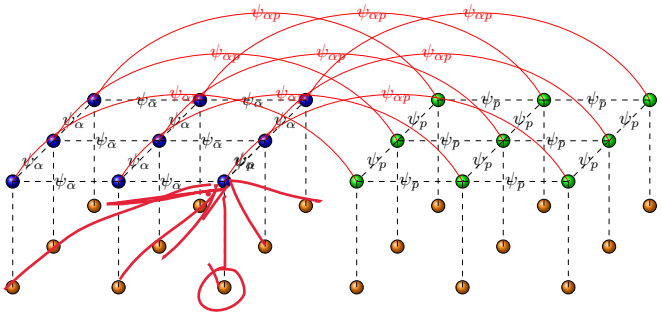

Fig. 3: Interaction between all the nodes from different sources V_1 and V_2 conditioned on the observed data - abundance and probability data (orange nodes).

3. DISCUSSION AND RESULTS

For our experiments we used the "AVIRIS Indian Pines" and "ROSIS-03 University of Pavia" hyperspectral images.

3.1. Indian Pines

The size of this scene is 145 x 145 with 220 bands in total with 20m spatial resolution in the spectral range from 0.2 to

Table 1: Average accuracies on the Indian Pines image

U	MLR	LC	MRFG	MRFL	CRFL
64.86 ±(3.4)	66.87 ±(2.7)	71.01 ±(2.28)	74.3 ±(5.2)	81.19 ±(4.2)	83 ±(4.2)

Table 2: Average accuracies on the University of Pavia image

U	MLR	LC	MRFG	MRFL	CRFL
63.04 ±(4.06)	65.72 ±(4.1)	68.6 ±(3)	73.6 ±(6)	80.76 ±(3.9)	82.11 ±(4.2)

2.3 μm. Prior to using the dataset, we manually discarded the noisy bands and the water absorption bands, leaving us with 164 bands. A ground reference map is available, consisting of 16 classes, from which we removed the smallest classes and used the rest for extraction of training and test pixels. The train data was composed of only 10 pixels per class. The value for the regularization parameter λ in the sparse unmixing problem (3) used to obtain the abundances was empirically selected as $\lambda = 4 \cdot 10^{-4}$. Afterwards the abundances were normalized. In the MRFL proposed approach the β parameter which weights the influence of the spatial term was set to $\beta = 0.5$ following the literature[x]. While the β, θ_b and σ parameters from the CRFL proposed approach are learned from the training data. The performance of our methods was compared with: the unmixing method used as a classifier (U) acting on the abundances as a single source, the MLR classifier acting on the probabilities as single source, the linear weighting approach using both abundance and probability sources and the MRFG approach fusing both sources as well. Table 1 shows that the proposed methods MRFL and CRFL outperform: 1) the first two methods U and MLR which are classifying the pixels without performing any fusion, they base their decisions solely on their individual sources 2) the linear combination of abundance and probabilities - LC method (the results using the original abundances are mentioned in this table, other transformations of these abundances gave us similar results) 3) the MRFG method (using the probabilities from the original abundances as features, as described here[x]) which fuses these 2 sources based on the certainty degree of the: a) class probabilities and abundances, b) the confidence scores exacted from the unmixing (as a classifier) and the MLR method.

3.2. University of Pavia

We performed the same experiments on the University of Pavia hyperspectral image with 115 bands, 610 x 340 pixels in the scene with a spectral range from 0.43 to 0.86 μm, with very high spatial resolution of 1.3 meters per pixel. Twelve noisy bands have been removed, and the remaining 103 spectral channels are used. The ground truth map consists of nine classes: Trees, asphalt, bitumen, gravel, metal sheets, shadow, self-blocking bricks, meadows and bare soil. As in the previous image, only 10 pixels per class were used as training data. The unmixing regularization parameter λ was set in similar manner as the previous experiment to: $\lambda = 4 \cdot 10^{-4}$, the abundances were normalized, the β parameter from MRFL proposed method is set to $\beta = 0.5$ following the literature[x] and the β, θ_b and σ parameters from the CRFL proposed approach are learned from the training data. Results can be seen in Table 2, where similar results can be observed as in the first image.

4. REFERENCES

[1] Chih-Chung Chang and Chih-Jen Lin, "LIBSVM: A library for support vector machines," *ACM Transactions on Intelligent Systems and Technology*, vol. 2, pp. 27:1–27:27, 2011.

[2] Mingmin Chi and Lorenzo Bruzzone, "Semisupervised classification of hyperspectral images by SVMs optimized in the primal," *IEEE TRANSACTIONS ON GEOSCIENCE AND REMOTE SENSING*, vol. 45, no. 6, 2, pp. 1870–1880, JUN 2007.

[3] Suju Rajan, Joydeep Ghosh, and Melba M. Crawford, "An active learning approach to hyperspectral data classification," *IEEE TRANSACTIONS ON GEOSCIENCE AND REMOTE SENSING*, vol. 46, no. 4, 2, pp. 1231–1242, APR 2008.

[4] I. Dopido, Jun Li, P. Gamba, and A. Plaza, "A new hybrid strategy combining semisupervised classification and unmixing of hyperspectral data," *Selected Topics in Applied Earth Observations and Remote Sensing, IEEE Journal of*, vol. 7, pp. 3619–3629, August 2014.

[5] D.C. Heinz and Chein-I Chang, "Fully constrained least squares linear spectral mixture analysis method for material quantification in hyperspectral imagery," *Geoscience and Remote Sensing, IEEE Transactions on*, vol. 39, no. 3, pp. 529–545, Mar 2001.

[6] J.M. Bioucas-Dias and M.A.T. Figueiredo, "Alternating direction algorithms for constrained sparse regression: Application to hyperspectral unmixing," in *Hyperspectral Image and Signal Processing: Evolution in Remote Sensing (WHISPERS), 2010 2nd Workshop on*, June 2010, pp. 1–4.